UNIVERSITY OF LATVIA FACULTY OF PHYSICS, MATHEMATICS AND OPTOMETRY



AINARS OZOLS

Optimization of materials, design and production technology of multifocal liquid crystal diffuser for augmented reality displays

SUMMARY OF DOCTORAL THESIS

Submitted for the degree of Doctor of Physics Subfield: Material Physics The doctoral thesis was carried out in EuroLCDs, the Institute of Solid State Physics, University of Latvia from 2020 to 2022.

The thesis contains the introduction, four chapters, conclusions, thesis and reference list.

Form of the thesis: dissertation in Physics, Material Physics.

Supervisor: Dr. phys. Martins Rutkis, lead researcher at the Institute of Solid State Physics, University of Latvia.

Reviewers: Dr. habil. phys. Janis Purans, Institute of Solid State Physics, University of Latvia, Dr. habil. phys. Maris Knitte, Riga Technical University, Dr. chem. Romaric Massard, eLstar Dynamics (The Netherlands).

The thesis will be defended at the public session of the Doctoral Committee of Physics, Astronomy and Mechanics, the Institute of Solid State Physics, University of Latvia, at 13:00 on 28th of November, 2022.

The thesis is available at the Library of the University of Latvia, Raina blvd. 19.

This thesis is accepted for the commencement of the degree of Doctor of Physics and Astronomy on 19. September, 2022 by the Promotion Council of Physics and Astronomy, University of Latvia.

Chairman of the Promotion Council	/ Anatolijs
Secretary of the council	Šarakovskis / Sintija Siliņa
	© University of Latvia, 2022 ©Ainars Ozols, 2022

Annotation

Aim of the promotion work is to design miniature, multilayer liquid crystal diffuser with improved electro-optical properties suitable for application in augmented reality head mounted displays. Investigate, characterize and analyse its construction materials as well as improvement capabilities.

Work tasks, established for fulfilling the aim:

- 1. Investigate literature data applicable to miniature liquid crystal diffusers;
- 2. Find optimum material combination and structural design for diffusers by using numerical modelling methods thus decreasing amount of experimental work;
- 3. According to modelling results, manufacture experimental diffuser samples and analyse obtained results, as well as evaluate reliability of modelling;
- 4. Perform scale-up of technology and ensure protection of intellectual property rights for innovations of this work.

Research outline for given goals are structured in four main chapters with sub chapters.

First chapter is devoted for characterization and performance analysis of multifocal diffusers, setting future target specifications for their form factor, switching speed, transparency and other important parameters for application in augmented reality displays. Second chapter is committed to active key element of diffusers – cholesteric liquid crystals. Analysis of switching mechanism is given that further allows optimization of functional properties. Method for determination of light refraction index dispersion for new, scattering type liquid crystal compositions as well as their layer thickness determination in diffuser applications are developed. Third chapter focus is on thin film properties and their stack design and optimization, starting from conductive indium-tin oxide and ending with broad band antireflective coatings. Numerical modelling methods have been used to decrease number of experiments for improvement of optical properties. In cases, where traditional materials cannot be used, new material investigation and application have been done, namely silicon oxynitride thin films with variable refraction index.

In the fourth chapter, modelling and experimental work was done to improve miniature multifocal diffuser production technology by using thinner glass substrates and less inactive structural elements (spacers).

At the end of the work, main conclusions are formulated and most important results are given, as well as problems with prosed solutions. Promotion work for doctoral degree is laid out on 165 pages. Work contains 44 tables, 142 figures, 1 addendum. 112 references to other works are given.

Contents

Annotation	3
List of symbols and abbreviations	5
Introduction	6
Motivation	8
Aim of the study	9
Author's contribution	9
Scientific novelty	10
1. Literature Background	10
1.1. Dynamic light scattering by liquid crystals	10
1.2. Diffuser solid state material interaction with light	13
1.3. Single diffuser and multifocal diffuser build up	14
2. Experimental	16
3. Results and discussion	18
3.1. Dynamic light scattering by liquid crystals	18
3.1.1. Switching mechanism	18
3.1.2. Optimization of LC spectral response	22
3.1.3. LC thickness and refraction index determination	24
3.2. Diffuser solid state material interaction with electromagnetic waves	s.25
3.2.1. Optimization of antireflective film stack on outer surface of	
diffuser	
3.2.2. Optimization of transparent conductive layer	
3.2.3. Dielectric coating	
3.3. Single diffuser and multifocal diffuser build up	
4. Conclusions	
Main thesis	
Authors list of publications	
References	44

List of symbols and abbreviations

	Ondinant nafaaatiya inday	DDAD	Broad band antireflective
n _o	Ordinary refractive index	BBAR	Broad band antireffective
n _e	Extraordinary refractive index	coating	Delaman stabiling d
Δn	Difference between ordinary and	PSCT	Polymer stabilized
	dinary refractive index		eric texture
P	Liquid crystal pitch	PDLC	Polymer dispersed liquid
P_0	helical pitch at zero field	crystal	B.1. 6. 11. 11 1
λ_0	Wavelength of light in vacuum	PFLC	Polymer free liquid crystal
ns	Nanosecond	PVD	Physical vapor deposition
nm	Nanometre	CVD	Chemical vapor deposition
nF	Nano farad	ODF	One drop fill
ps	Picosecond	RGB	Red Green Blue color
μs	Microseconds	model	
mg	Milligram	FC-D	Metastable focal conic
μg	Microgram	state	
VR	Virtual reality	HTP	Helical twisting power
AR	Augmented reality	E7	LC reference composition,
3D	Three-dimensional	Merck t	rade name
VAC	Vergence-accommodation	XPS	X-ray photoelectron
conflict		spectros	scopy
MOE	Multi-plane optical element	DC	Direct current voltage
LED	Light emitting diode	sccm	Standard cubic centimetres
LCD	Liquid crystal device	per min	ute
LC	Liquid crystal	VCF	Vacuum capillary fill
DSM	Dynamic scattering mode	method	•
P	Planar state	UV	Ultraviolet spectra
ITO	Indium tin oxide	AA	Active area of display
FC	Focal conic state	Pcs	Pieces
TP	Transient planar state for PDLC		
M	Transient state for PFLC		
Н	Homeotropic state		
TN	Twisted nematic		
E-O	Electro-optical (response)		
	zittas opticai (response)		

Introduction

Demonstrated on the brink of the 20th century by Ferdinand Braun [1], the cathode ray tube was the first widely used display technology. In the past decades, the liquid crystal displays (LCD) have become the market dominant technology – in 2019, almost half of private households worldwide were estimated to have a personal computer and in developed countries, this number is closer to 80 percent [2]. Even though many people spend their entire working-days looking at some form of digital display, the displays themselves have not undergone a major paradigm shift since their inception – the majority of displays still render a 2D image on a flat surface. Some efforts have been made towards displaying 3D images, but that has predominantly been achieved by use of stereoscopic 2D displays with binocular disparity. The problem with such an approach is the perceived ambiguity in 3D graphics representation due to the lack of true depth cues. This issue can be solved by utilization of a volumetric display.

There are multiple approaches of implementing a volumetric display, but the general concept is image generation from light-emitting, scattering or relaying pixels (called voxels) that occupy a physical volume in space [3]. A volumetric display can be either static (solid-state up-conversion displays, gas medium displays, voxel arrays, layered LCD stacks, and crystal cubes) as well as swept (rotating LED arrays, cathode ray spheres, varifocal mirror displays, rotating helix displays, and rotating flat screens) [4], [5]. The swept volume displays make use of the persistence of human vision to recreate 3D images. While a multitude of elaborate methods (e.g., the photophoretic-trap volumetric display [6]) for creating a volumetric display has been demonstrated in laboratory conditions, many of these display types are far from market-ready due to the complexity of manufacturing, safety concerns, low image resolution, low refresh rate or sub-par colour reproduction.

The majority of currently-feasible volumetric displays are based on rear-projection and some sort of screen (either static or swept). The major limitation for these kinds of displays is the frequency of operation of the projection unit — this means finding a compromise between the total volume of a display and its discretization (the number of layers). Even though volumetric displays with moving membranes/screens have reached a stage of development past a laboratory demonstration [7] and can be considered commercial product-ready (e.g., the Voxon VX1), the lifespan of devices with moving parts are usually shorter than that of their solid-state counterparts. Therefore, the preferred implementation of a volumetric display is often entirely solid-state, and swept displays are mostly used for niche products. A proposed solution for an entirely solid-state display is a stack of transparent organic light-emitting diode (OLED) panels [8], however, the transparency and haze values do not currently allow reaching a meaningful stack depth. Alternatively, a rear-projection device

coupled with a stack of fast-switching liquid crystal (LC) diffuser elements can yield in a practical volumetric display with reasonable volume and its discretization. This concept has been researched in-depth [9] at LightSpace Technologies/EuroLCDs and the focus of this work is to provide comprehensive analysis of solid-state volumetric display architecture and the required properties of the corresponding key-enabling element – a liquid crystal diffuser.

3D displays of future with certainty will have to overcome limitations of currently common stereoscopic 3D displays – such as used for virtual and augmented reality. It could be said that the main shortcoming of single-focal plane stereo displays is lack of consistency between vergence and accommodation depth cues – in other words, a viewer has to fixate accommodation at a single distance. This brings about well-known by now vergence-accommodation conflict which can manifest differently for different people but most commonly is associated to eye-strain, blurry vision and generally contributing to what is known as "cyber-sickness" [10], [11].

A very promising solution for enabling consistent accommodation within a 3D scene presented by a stereoscopic display – is solid-state multi-focal displays [12]. While implementations with varifocal lenses have been demonstrated [13], [14], a solid-state solution typically is regarded as more preferable. For a solid-state implementation a stack of transparent displays is needed. Previously it was believed, that such candidate would be a transparent OLED display [15], [16]—nevertheless, endeavours of researchers and manufacturers didn't succeed to an expected extent. One of the main drawbacks was optical haze, which prevented formation of screen stacks and generation of high-quality image.

Thus, a very viable alternative concepts of which have been demonstrated in early 2000s is a solid-state volumetric technology based on switching optical diffuser elements [9]. The early implementation was based on polymer-dispersed liquid crystal (PDLC) of cholesteric type. Under applied voltage cholesteric spirals were broken up and liquid crystal transitioned into a homeotropic state (H) having high transparency and low haze values. Upon removal of voltage – it collapsed back to light scattering focal-conic state (FC) [17]. The addition of polymer network helped with FC domain formation and generally improved light scattering properties in the diffuse state. Nonetheless, presence of polymer network within a diffuser element interfered with incident light in the transparent state – having unwanted haze off the principal view direction. In terms of switching characteristics, polymer networks also tend to slow-down the transition between optical states, which is crucial for multi-focal and volumetric display architectures reliant on a time-sequential switching between multiple stacked diffusers.

To overcome these limitations a diffuser composition without addition of stabilizing polymer networks was developed. A polymer-free liquid crystal

(PFLC) of cholesteric type cell works similarly to PDLC cells in a time-sequential display scenario. Instead of polymer networks facilitating scattering of light, the relatively short-lived transient super scattering state (FC-D) is utilized. This state is characterized by fine-domain structure of focal-conic (FC) texture, which isn't stable [18] for long periods but more than sufficient for time-scales required by time-sequential switching in a volumetric display.

The task of this work has been to redesign PFLC cells for new application in head mounted, volumetric augmented reality displays. New requirements demand to investigate liquid crystal switching mechanisms and optimize overall design of the cell for optimized optical performance of small form factor application. Rather than simply downsizing, the strategy towards this task is to design from set requirements, use modelling approach to decrease experimental work volume and modify existing materials and methods or develop new materials.

Motivation

The journey to this work started in 2011 when founder of EuroLCDs company, Ilmars Osmanis said: "We have 27 trucks of LCD equipment and agreement from Ventspils Free Port Authority for green field project. It is your task to build factory, develop technology, hire and train staff so we can produce liquid crystal devices for 3D volumetric image devices". I had relevant industrial experience but the display technologies were known to me only by general principles and education in organic chemistry.

So it began, from designing cleanroom and factory, to first 80x80 mm LCD trials to 19-inch diffusers, then to 27-inch displays, mostly developing technology by ourselves. We gathered information on LCD technology from books, publications and many people who provided guidance in this journey. It will be a very long list of sources, names, companies and research institutions. As we begin to specialize in large size, high voltage, scattering type of displays, the technology started to differ from traditional LCD technology. Stepwise we adapted it for larger and larger sizes, mostly based on experimental data.

In 2019 the focus changed to small displays with the trend towards head mounted displays. This provided new challenge, as microdisplays demands other materials and technologies. This time we wanted to start with the design, select proper materials for expected outcomes, reduce number of experiments by modelling the solutions, a more proper way to design new product. I was going to review my current knowledge and material physics. As with COVID-19 lockdowns, more time was available for writing, I decided to summarize findings in form of PhD work. With this work, I hope to fill the gaps in my knowledge and in the same time leave valuable knowledge for my colleagues for years to come.

Moreover, the application of augmented reality head mounted displays for professional medics become important due to higher demands for safety from COVID-19 infections. The benefit of augmenting reality in operation rooms and hospitals for medics without contamination risks was clearly seen by professionals. PFLC diffuser technology proven for large form factor volumetric displays, at this time point, was the one that could be developed this application.

Aim of the study

Is to develop key enabling element for multi focal display application by downsizing PFLC diffusers by:

- investigating literature data applicable to miniature liquid crystal diffusers:
- characterizing material properties for application if literature or supplier data is not available;
- find optimum material combination and structural design for diffusers by using numerical modelling methods thus decreasing amount of experimental work;
- according to modelling results, manufacture experimental diffuser samples and analyze obtained results, as well as evaluate reliability of modelling;
- if traditionally used materials and methods are not capable to provide expected results, research new methods and materials for improving diffuser electro optical performance, namely transmittance of the open state, scattering properties of closed (diffuse) state and minimize switching time between both states;
- find the best diffuser design based on literature review and experimental results;
- perform scale-up of technology and ensure protection of intellectual property rights for innovations of this work.

Author's contribution

The experiments presented in this work were done by the author of this work, except specific experiments and measurements with equipment available in Institute of Solid-State Physics that required proper training and qualification (XPS, AFM, sputtering cluster etc.). Characterization of diffuser visual properties with combination of headset projection system were done by my colleagues in Lightspace Technologies.

The author prepared Design of experiment plans for the work, supervised operations and prepared reports using liquid crystal display production line. Line functions were ensured by its operators. If multiple sample

characterization were required, it was done by operators, using methodology developed by author after first samples have been tested. All COMSOL Multiphysics, CODE V modelling were done by the author. Optilayer and Filmwizard modelling were carried out by colleagues Martins Narels and Sandra Balode.

All of the data processing and result interpretation were done by the author.

Scientific novelty

A novel PFLC diffuser element system (optical chip) was developed in small size factor, enabling its use in AR-HMD systems. For a first time SiO_xN_y coatings were used to improve optical performance of the diffuser element as index matching, dielectric and LC orientational layer. Switching time was improved by means of optimizing high twisting power dopant concentration and surface alignment combination and spectral dispersion of diffuse state. For a first time it was demonstrated that switching happens through uniform lying helix.

A demonstration unit of diffuser element has been made and is successfully integrated in AR-HMD system.

Completed research and implementation work have been included in the 4 patents and 3 more patent applications are currently submitted.

1. Literature Background

1.1. Dynamic light scattering by liquid crystals

The main operational part of the display is the liquid crystal, the material that exists between conventional isotropic state (liquid) and three dimensionally ordered solid crystal with only orientational order but no positional order. In the displays, the most important is that its optical properties can be directed by external electric field [1] and the low viscosity means that optical properties can be changed by relatively small force and fast.

In this work, the focus is on cholesteric LC that scatter unpolarized light in one state and be as much as possible transparent in other, and can be switched from one state to other as fast as possible. Cholesteric LC are composed by chiral molecules and they were next LC type that was used for light scattering. Initially first discovered were cholesteric molecule derivatives, giving the name of class. Cholesteric LC can be composed by chiral nematic molecules or formed by adding chiral dopant to nematic LC mixture. Twist in LC structure happens with alignment between molecules with slight angle to one another producing quasi nematic layers. Their individual directors are turned by a fixed angle form one layer to another. The pitch (p) is the distance over which the

director of LC molecules undergoes a full twist of 2π angle. As the phase directors at 0° and 180° are equivalent, the arrangement of molecules in the chiral nematic phase repeats at every half pitch (p/2), see *Figure 1*. Due to this strong twisting effect, cholesteric LC shows a selective reflection of the circularly polarized light of wavelength equal to pitch length [2].

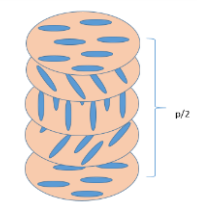


Figure 1 Cholesteric pitch formation

The cholesteric mode has two distinct stable states, the planar (**P**) and focal conic (**FC**) states. In planar state, all helical axes align normal to the surfaces. In this state, it is Bragg reflector [3], see Figure 2.

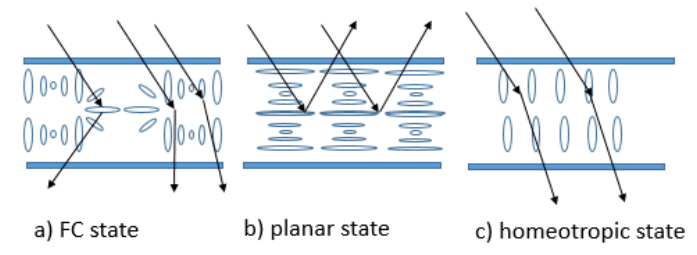


Figure 2 Focal Conic (a), planar state (b) and homeotropic state (c)

Upon application of electrical field, the change from planar to focal conic state happens. The texture is strongly forward scattering and selective reflection property vanishes. Polymer network is typically used for state stabilization (polymer stabilized (PSLC) or polymer dispersed (PDLC) modes) but introduces haze due to refractive index mismatch.

If electric field is slowly decreased, transition back is not homogenous, but instead is nucleation process that starts at defects in the sample such as spacers or polymer network within bulk LC volume. The focal conic texture grows from just a few places so it forms larger domains. If the voltage is removed suddenly, the domains form in many more places at once and therefore the average domain size tends to be smaller, which results in better light scattering [4]. This transition has been studied and found, that it happens through transient planar scattering states (**TP**) [3]. There is also the fourth state, homeotropic (H) induced by electric field where no twist happens and all directors are pointing

perpendicular to the substrate plane. Surface alignment of LC (planar or homeotropic) do not influence the time needed to switch from the **TP** state to the **P** state [5].

Polymer-free Cholesteric (PFLC) Liquid mode was first described in patent [6]. The electric field untwists the chiral nematic or cholesteric liquid crystal molecules and homeotropically aligns the liquid crystal directors to transform the liquid crystals into a transparent homeotropic state. When electric field is turned off, the liquid crystalline material forms microdomain textures and scatters light. Authors claimed that, although the directors within each microdomain are ordered (i.e., short range order), they are disordered with respect to other microdomains. This localized chiral domain formation was believed to contribute to the observed transient scattering effect.

PFLC cells, can be considered as evolution step of PDLC cell [7]. The polymer structure inside cell is absent and faster switching speeds are observed as well as improved scattering properties, see Figure 3. PDLC cells use relative long cholesteric pitch, whereas for PFLC very short pitch <500nm is required. Polymer free and PDLC diffuser E-O responses are similar, except for transient increase of transmittance **M** during transition from clear to scatter state.

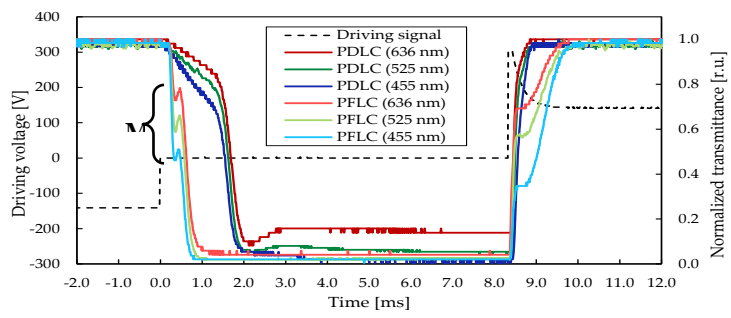


Figure 3 Dynamics of electrical and optical signals for PDLC versus PFLC diffuser with a 15µm active LC layer measured with 3 wavelength laser system

The minimal transmissive state (transient focal conic) is not stable and scattering state degrades over time into static focal conic state. This limits PFLC uses for short light diffusing periods. The later research studies [8] for these diffusers proposed that transition from clear homeotropic state (**H**) to diffuse focal conic (**FC**) state happens through metastable planar state (**TP**), in analogy to PSCT, as transient raise of transmittance is observed.

LC, like any material in optical device, must be characterized for device design and optical performance optimization. LC refraction index (RI) dispersion over spectra can be measured by multi-wavelength Abbe refractometer [9] or using the spectral reflectometry method [10]. The spectral reflector meter processes the light spectrum reflected or permeated by the sample. If the sample consists of a multilayer system in which multiple internal reflections occur, the interference bands may be observed in the spectrum, whose position is determined by the optical properties of the investigated layers - thickness and refractive index. In the Institute of Solid State Physics this method is used to determine the refraction indexes of 1 μ m thick layers [11].

In the same time, unlike solid materials used in LCD construction, LC layer thickness can vary. Methods for determination cell gap using light polarization are well developed and commercially available but does not work for scattering type or other special type LCDs [12]. Spectroscopic method can be used to measure LC layer thickness based on transmission spectra measurements where interference is created by different layers with different thicknesses and refractive indexes. By using mathematical methods, cell gap and RI can be calculated from transmittance spectrum [9]. Yet this requires the refraction index to be known first. If gap (layer) is filled by air instead of LC material, the interference peak determination is easy but it is commonly known in the industry that cell gap for unfilled displays is larger than for filled displays, up to 20%.

1.2. Diffuser solid state material interaction with light

The first boundary light (electromagnetic waves) from image projection system meets is air/glass. Whenever boundary of different refraction index materials is used, reflections according to Snell law appear. Common approach to reduce reflections is by designing antireflective layer stack. There are known methods for calculating antireflective layers, starting from matrix transfer method to Fresnel equation [13].

COMSOL Multiphysics have Geometric Optics module with built-in Maxwell and Fresnel equations and can be used for this task using finite element method. Diffuser manipulates electromagnetic waves in visible range by arranging LC molecules with applied electric field by transparent thin conductive film, typically indium tin oxide film (ITO) on both sides of LC layer so that they are passed through or scattered. Contrary to the traditional LCDs where active area is made of many small pixels, diffuser has one large pixel that must be uniformity charged at high electrical field intensity so high conductivity could be preferred. However, higher conductivity typically means thicker layer which is less transparent. In the same time diffuser must be highly transparent for visible range electromagnetic waves, so thin layer could be preferred, so a compromise must be found.

ITO properties can be changed to some extent. Typically, ITO is sputtered on glass by physical vapor deposition (PVD) technique at substrate temperatures above 300°C with slight oxygen deficit. Coatings at these temperatures have

best conductivity due to crystalline lattice structure and oxygen vacancies in addition to built-in tin ions. It is possible to deposit ITO at lower temperatures and later use thermal treatment at 300°C at reductive atmosphere but conductivity will be lower at least by factor of 2 [14]. This is common solution for sample production or sputtering on temperature sensitive substrates, like polyethylene terephthalate (PET) films. If higher temperatures and oxidative conditions are used, for example for next process steps, conductivity will decrease due to incorporating oxygen into structures [15].

Dielectric insulator layer on top of transparent conductive must provide following functions [3]:

- Align LC molecules in certain direction;
- Even out electric field across transparent conductive electrode area;
- Be as thin as possible so the main voltage drop happens across LC layer;
- Prevent the capacitor structure from shorting;
- Its refractive index should be matched to adjacent layers to minimize internal reflections.

Traditional LCD organic alignment materials [16] generally provides good correspondence to first three points, while fast switching requires high voltage which is not typically addressed in common LCD modes but increases importance of fourth point. Moreover, for micro displays, inorganic materials are preferred, as there is high-power arc lamp illumination. Short wave blue light lead to differential aging in multiple-micro display projectors, distorting colors [17]. Current approach to readily available range of commercial compounds would be utilization of magnetron-sputtered thin films. In previous work it has been shown, that traditional LCD materials as SiO₂ and polyimides can be replaced by SiO_x thin films deposited by magnetron sputtering [18] as they exhibit high transmittance and high resistance to dielectric breakdown. Moreover, it is possible to adjust the refractive index of magnetron-sputtered films by varying deposition parameters. For example, SiO_xN_y is very suitable dielectric material for optical diffuser applications, since it's refractive index can be varied from 1.5 to 2.0 [19].

1.3. Single diffuser and multifocal diffuser build up

Historically first method for LCD cell assembly was to assemble top and bottom substrates with coatings in atmosphere, cure gasket and then fill LC inside the formed cells. The fill process starts by vacuuming the cells through hole in the gasket and adding LC to it afterwards, thus called vacuum capillary fill (VCF) method. Due to narrow cell gap, LC first enters the cell under capillary forces and then under force of atmospheric pressure. Cell gap is not perfect, it is typically overfilled. Cell is then pressed to squeeze out excess of LC and sealed. Method works well for certain sizes, as for large sizes it takes

too long time to fill while LC mixture evaporates. To overcome this limitation, "one drop method" (ODF) was invented, so one or many drops of LC were placed inside closed gasket and both substrates were assembled in vacuum. The cell gap accuracy in this case depends on dispensing accuracy but method allowed display production above 21-inch sizes [20]. This is also convenient method for smaller displays as handling operations are reduced.

Gap between two dielectric layers with electric field must be precisely controlled as its thickness determines electro - optical properties, typically in the range of 2 to 50 micron. As it will be filled with liquid crystal layer, which as liquid is not compressible and can provide cell gap control by itself, anyway, for cell construction certain means of cell gap control are needed [21]. This is achieved by depositing spacers or making support structures photolithographic means. Spacers can be placed outside active area (mixed in gasket material and then dispensed) and on active area by spray. Spacers can be made from glass or polymer (radical polymerization of styrene and divinylbenzene). Both are inert to LC but polymer is preferred because their thermal expansion is similar to that of liquid crystal, and is compressible. Depending on pixel size, spacer takes away affective active area, resulting in light loss or visible artifact (depending on magnification). This becomes very important for micro displays where spacer can block half of pixel. Thus, to improve efficiency spacers should be absent or kept at minimum only to ensure mechanical support during manufacturing or use [21].

During ODF process, top and bottom coated substrates are joined in vacuum by 8 kg force. This is enough to press the gasket with mixed spacers to designed cell gap. The substrate above display active area at this moment rests on spacers. Small unfilled gap is present as 95±2% of LC fill ratio is used as gap limiting factor. Alternatively, if classic liquid crystal vacuum filling is used, spacers must be present, that during end seal process, exact cell gap can be adjusted by pressing LCD sides. Spacers elastically deform to precalculated size and ensure constant gap within display series [22].

Spacer density depends on required cell gap, accuracy and LCD type. The most common density values are 10 to 200 spacers per mm². One method [23] is to calculate the spacer density based on their compressibility. In general, it is recommended to compress at least 5% that when liquid crystal volume expands at elevated temperatures, spacers stay fixed.

For micro-displays due to their small size there is possibility for "spacerless" approach, so the gap uniformity is ensured by either gasket or precise amount of liquid crystal inside the cell. The disadvantage of this "spacerless" method is that the uniformity of the cell gap depends on the flatness of the substrates [24], [25] and LC dispensing accuracy.

Spacer distribution uniformity requirement is dependent on LCD type, for example STN type will require 4.2±0.1 of gap accuracy. The requirement for diffuser type LCD is less, a 10% accuracy will be sufficient.

2. Experimental

Diffuser cells with corresponding cell-gaps of 4-25 microns were prepared using two 0.55 mm thick plane parallel glass substrates separated by divinyl-benzene spacers. The glass substrates were coated by thin transparent conductive layer of indium tin oxide (ITO) with the corresponding sheet resistance of 80 Ω/\Box . Surface alignment layers were prepared from commercially available poly-imide materials from Nissan Chemicals by flexoprinting method. Alternative alignment layers were prepared from Si targets in oxygen atmosphere using physical vapor deposition (PVD) equipment or chemical vapor deposition (CVD). Rubbing was used to provide directional alignment with rayon cloth if cell design required preferred LC orientation. Cells were assembled in industrial LCD manufacturing line by using one drop fill (ODF) technology. Nematic liquid crystal mixture was doped with optical dopant having high helical twisting power. Concentrations of the chiral dopant were higher than typically used in PDLC technology, and were initially dissolved in acetone, then mixed with liquid crystal mixture and refluxed for several hours to remove acetone. Electrical connections were attached to ITO layer by means of ultrasonic soldering to keep contact resistance minimal. Electro-optical response of the devices was characterized by VST-1 (white LED light source), VST-2 (3 laser beam system of wavelengths 635 nm, 532 nm, 450nm), VST-3 (synchronized spectrometer). Haze measurements were carried out using CHN Spec Haze Meter TH-100. A programmed voltage waveform from the lock-in in-built function generator was amplified and then applied to the electrodes (ITO glasses), see Figure 4. If not noted specifically, 0.1 ms overdrive length was used to facilitate faster switching. Drive voltage is supplied for 8.33 ms.

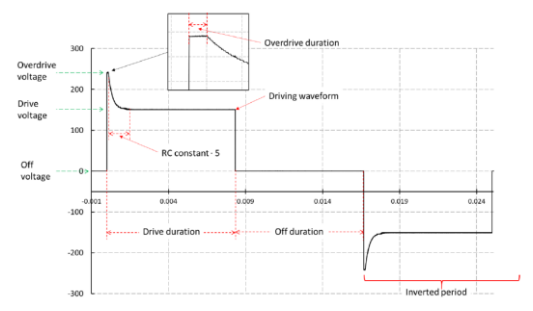


Figure 4 Typical waveform used for characterization

Industrial coater FHR Line2500.H was used for layer deposition on 400x300x0.55mm soda-lime glass by physical vapour deposition method. Silica and nyobium oxide rotable targets and ITO planar target were used in reactive oxygen/argon atmosphere. Prior deposition, to ensure cleanliness of the surface, ion etching was used with following parameters: 50 mm/s, 4 passes under target and Argon flow at each of 3 sections – 250, 40, 150 sccm. After each layer was deposited, sample was collected and its thickness was measured by Dektak XT profilometer using Vision 64 software. Transmittance and reflectivity were measured by Ocean Optics Flame T spectrometer. Approximately 2-3 experimental runs per layer were necessary to reach specified thickness by changing glass conveyor speed under target (process speed, mm/s) and number of passes under target (number of cycles). Parameters that were kept constant – 4.85x10⁻⁶ bar, process temperature 58 °C, rotation speed of target 15 mm/s, DC power 15 kW, 675 V and Ar flow at 3 sections – 900, 150 and 450 sccm. Oxygen flow for Nb₂O₅ process was set to 95 sccm and for SiO_x it was increased to 102.1 sccm for stable process. Oxygen flow for ITO process was 18 sccm.

Pilot scale SiO_xN_y coatings were prepared on soda-lime glass using BDS-HF200/300 BDISCOM Srl RF magnetron sputtering system. Target material for SiO_xN_y sputtering was Si₃N₄ with 99.999 % purity, 3 inches in diameter and 6 mm in thickness. For all samples following parameters of magnetron sputtering were constant: power (100 W), distance between target surface and substrate (11.5 *cm*), pulsed DC frequency (100 *kHz*), pause duration time (3 μ s).

3. Results and discussion

3.1. Dynamic light scattering by liquid crystals

3.1.1. Switching mechanism

For a typical cholesteric (long cholesteric pitch) LC crystal cell, the switching behavior is dependent on the driving voltage (electric field intensity) — with the increase in voltage the rise time shortens but the opposite process or fall time expands. In contrast, for PFLC cells (with short cholesteric pitch) a fall time is virtually independent of the driving voltage.

The polymer-free variant of a LC cell typically facilitates faster state-transitions from FC to H state due to lack of additional polymer-LC interfaces translating into improved overall transparency without sacrificing the scattering properties. Increasing the driving voltage reduces the time of transition from the FC state to the H state, however it also increases the likelihood that the LC cell will undergo electrical breakdown, especially when threshold voltage is already high. With suitable dielectric breakdown prevention measures, driving voltage can be increased few times and rise time can be shortened, even up to 6 μ s.

However, this is not possible for a fall time of a transition from the transparent **H** state to the **FC** state, as it depends on the particular LC formulation (will not be addressed here as it was optimized before this work) and chiral agent system as well as the geometric dimensions of a diffuser-element.

In \mathbf{H} state an electric field ensures that the elastic energy of induced cholesteric LC, is compensated by an electric field. Increasing a concentration of dopant will change a helical pitch P_0 , thus storing more elastic energy in a spiral of cholesteric LC, as the result fall time should decrease. As we can see from results see *Table 1*, after maximum scattering is achieved, there is maximum workable concentration, after which switching time increases again and later scattering start to decrease, due to oversaturation by the dopant. It should be also noted that for such oversaturated systems switching speeds slow down most likely due to increased viscosity of the mixture and recrystallization of a dopant within a cell. Obviously, dopants with high helical twisting power (HTP) are preferred as this allows lower concentrations to be used. S-5011 is one with of the highest available HTP and is used here.

Dopant S-5011	Clear state	Scatter state	Fall	Raise
concentration,	transmittance,	transmittance,	time, us	time, us
w%	%	%		
0	86.4±0.2	85.5±0.4	527±271	0±56
0.5	87.0±0.2	86.0±0.2	857±407	3±0
1.0	86.3±0.2	67.1±0.1	519±6	116±6
1.5	77.9±1.2	36±2	1219±4	2720±68
2.0	87.2±0.4	3.0±0.1	1118±8	1631±9.2
2.5	85.9±0.2	2.3±0.3	756±5	1727±24
3.0	87.3±0.1	5.7±0.1	543±0	1884±22

For PFLCs if the electric field is decreased slowly, for example by discharging conserved electric energy through switched off driver unit or added resistor, the speed is slower and scattering **FC** state is never observed, transmission is only reduced to 40%, see *Figure 5*.

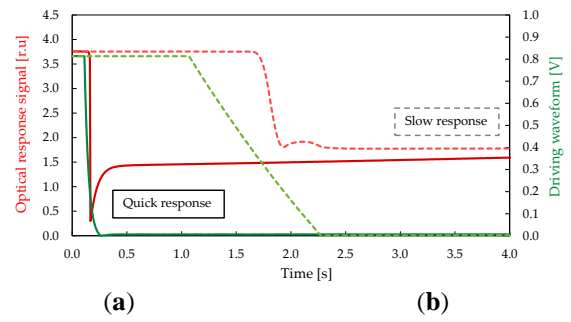


Figure 5 Electro optical response of diffuser, discharged a) fast and b) slowly through resistor. Note that slow discharge decreases scattering state significantly

The shortest switching time is observed when PFLC is discharged by short-circuiting but then the transient peak M is observed, see *Figure 3*. Approximately 0.2 ms are lost that can be potentially saved if its origin is understood.

As known from the literature, direct transition from **H** to Grandjean texture (the so-called planar state (**P**), with helix axis along the confining substrates normal) is not possible. Usually this transition pass through transient **FC** state. The cholesteric liquid crystal devices may exhibit three stable states with textures being Grandjean (**P**), Focal Conic (**FC**) and Uniform Lying Helix (**ULH**), respectively (see *Figure 6*).

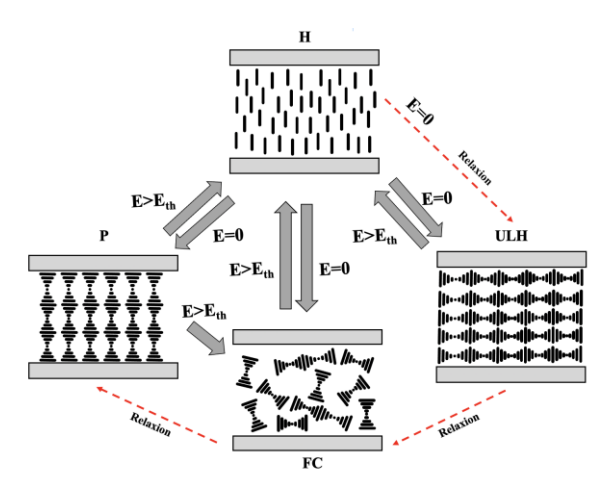


Figure 6 Schematic presentation of the structural transition in cholesterics. Transition from H to P state may involve transient ULH state in the relaxation process.

The switching between these states is possible by applying an electric field with appropriate form and duration, and/or surface treatment. Moreover, such a switching may be performed by application of mechanical flow with or without application of an electric field, which can be ether unidirectional, inducing transition from **P** or **FC** texture to **ULH** texture, or mechanical pressure inducing transition from **P** or **ULH** texture to **FC** texture.

The optical appearance of **P**, **FC** and **ULH** differs substantially. **P** texture is reflecting selectively the incoming light with wavelength λ_0 which is directly related to the cholesteric pitch p by $\lambda_0 = \Delta np$ where Δn is the average refractive index $[n = (n_0 + n_e)/2]$, with n_0 and n_e being the ordinary and extraordinary indices of refraction. **FC** texture is scattering the incoming light, whereas **ULH** texture is completely transparent.

Transitions between these textures with or without applied field is usually taking place through transient states (structures). In ref. [26], it was found appearance of transition peak M in the electro-optical curve after removal of the applied electric field during **H-P** transition, indicating an increase of the light transmission. The peak was considered to be a result of appearance of transient Grandjean-like cholesteric structure during the relaxation process.

A similar peak in the light transmission curve of the liquid crystal diffuser studied in this work, was obtained after removal the electric field. This peak **M** in the optical response of the liquid crystal diffuser is worsening the light scattering characteristic of the diffuser. The investigations show, see, however,

that the transient peak **M** doesn't exhibit selective reflection and therefore could not be assigned to appearance of a transient (**TP**) state, see *Figure 7*.

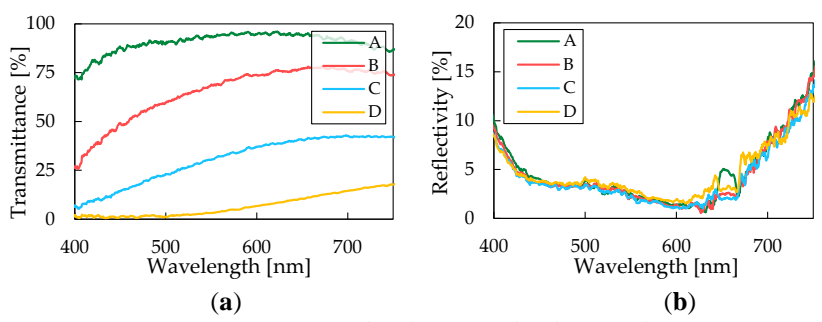


Figure 7 Transmittance (a) and reflectance (b) changes during various time points for 12-micron diffuser cell during fall. A – before transient peak, B – at transient peak, C – after, and D – at FC state

The increased light transmission, at the time of appearance of the peak **M**, suggests that formation of domains with uniform lying helix texture, which are optically transparent, takes place during the relaxation process. The material flow, which is a result of the structural changes in liquid crystal bulk, is considered as the origin of this transient state manifested by the peak **M** in the optical response of the diffuser. This flow may have parallel component with respect to the confining substrates in certain regions of the liquid crystal bulk. However, such a flow gives a preferred orientation of the growing as well as of the orientation of existing cholesteric domains, thus forming domains with transparent **ULH** structure. This process is transient and overgo with the time to **FC** state and then to **FC** state, respectively (see *Figure 6*, red arrows). Notice also that **H** texture may relax permanently to Grandjean texture through transient textures being either **FC** or **ULH**.

The appearance of transient **ULH** state, indicated by the peak **M** in the optical response of the liquid crystal diffuser, is not desirable. One possible way to remove it is to apply electric field with form of continuous decrease of the applied voltage (ramp) to the diffuser rather than a sudden switch-off the voltage but must be precisely in time with **ULH** state.

By changing anchoring conditions in the experimental cells, that promotes high reverse pretilt of the liquid crystal molecules at the confining substrates (pi-cell configuration), which eliminates the back flow effect in the \mathbf{H} state, shortening of the fall time was obtained.

Table 2 Surface impact on 7µm diffuser E-O test results (525 nm wavelength)

	Alignment conditions	Pretilt angle	Orientation	Rubbing length, m	Open, %	Close, %	Fall, µs	Rise, µs	Fall speed, %/µs
L	homeotropic	-	vertical	-	83.4	11.9	898	1322	0.080
=	planar	1ow	parallel	-	87.6	6.7	1001	1535	0.081
\leftrightarrows	planar	medium	antiparallel	1	88.5	6.4	1075	1807	0.076
⇉	planar	medium	parallel	1	87.8	6.7	1028	1517	0.079
⇉	planar	medium	parallel	16	87.0	6.4	991	1578	0.081
⇉	planar	medium	parallel	28	83.7	6.5	996	1541	0.077
<u>_f</u>	tilted	High	parallel	-	92.5	6.7	1046	1510	0.082

Another alternative way of shortening the response fall time is to accelerate the relaxation process by increasing the concentration of the nucleation seeds either in the liquid crystal bulk (*via* addition of nanoparticles or creating shallow appropriate polymer network) or by increasing their concentration on the substrates (creating appropriate surface topography).

3.1.2. Optimization of LC spectral response

For accurate colour representation, a diffuser element, in an ideal case, should absorb (as well as scatter) all wavelengths in the visible spectrum equally well. As can be seen from the transmission spectra in *Figure 8*, this is not the case – the diffuser-elements are more transparent to longer wavelengths of visible light in both the **H** and the **FC** states. This means that some colour adjustments are required when rendering an image if accurate colour representation is needed as the images otherwise appear reddish in colour.

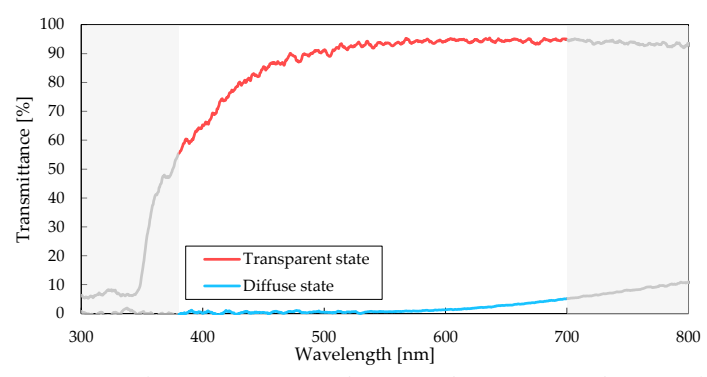


Figure 8 Spectral transmittance in diffuse and transparent diffuser-element states

Since in scattering state, when some part of the light is still transmitted, source of light can be seen and due to this effect, the "hotspot" has red color and is characterized as "red bleed-through". We can try to even out its spectral characteristics with dyes, used in LC industry for specific modes. Dye molecules can be turned with LC molecules, so color intensity is dependent on LC molecule orientation.

From spectral transmittance results of dye doped LC cells, see *Figure 9* we can see that none of added dyes have changed values at colour specific wavelengths compared to undoped reference but have increased scattering properties at larger wavelengths by increasing size of scattering domains, thus have improved contrast of diffusers.

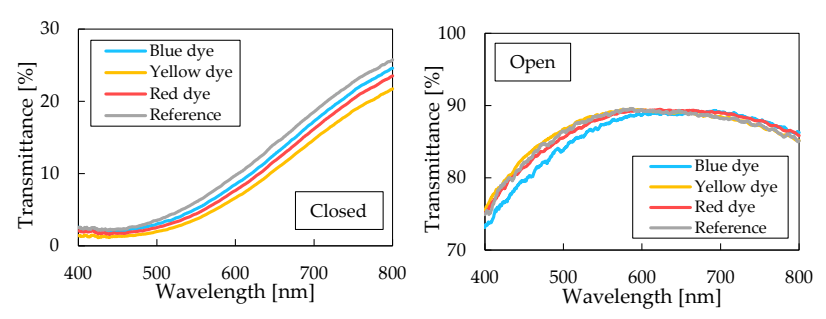


Figure 9. Spectral transmittance in diffuse and transparent diffuser-element states with doped dyes.

3.1.3. LC thickness and refraction index determination

To use spectroscopic method for further cell gap measurement of diffuser displays, refractive index must be known. To determine it, layer thickness of LC must be known first. If we take precautions that displays produced in the same conditions have the LC layer thickness, and fill some of them with "E7" liquid crystal mixture with known refractive index for thickness determination and some with diffuser LC, we can determine refraction index of later.

Displays were prepared in one batch, so one assumes, that all test displays have equal LC layer thickness but unknown absolute value, somewhat different from spacer size of 2.7 μ m. Capacitance measurement can be used to evaluate correctness LC layer thickness (cell gap) as it allows to compare one device to another. Diffuser and "E7" display capacitive structure simulation model was built using COMSOL Multiphysics software, see *Figure 10*.

Material	Thickness d, nm	Refractive Index n	Relative dielectric permittivity
Air	-	1.00	1.0
Glass	550000	1.52	7.75
SiO ₂ barrier layer	20	1.52	2.18
ITO conductive layer	30	1.82	-
Silica based hard coat	95	1.75	14
PI alignment layer	55	1.58	3.6
LC layer	8000	1.71	9.6
PI alignment layer	55	1.58	3.6
Silica based hard coat	95	1.75	14
ITO conductive layer	30	1.82	-
SiO ₂ barrier layer	20	1.52	2.18
Glass	550000	1.52	7.75
Air	-	1.00	1.0

Figure 10 Capacitative and resistive structure of diffuser. Refractive index and permittivity data from supplier data sheets. On the left, glass and LC layer thickness is not shown on scale, indicated by zig-zag white lines

Using LC layer thickness calculated for samples with E7 LC, refractive index of diffuser LC was calculated and average n calculated, see values plotted in *Figure 11*.

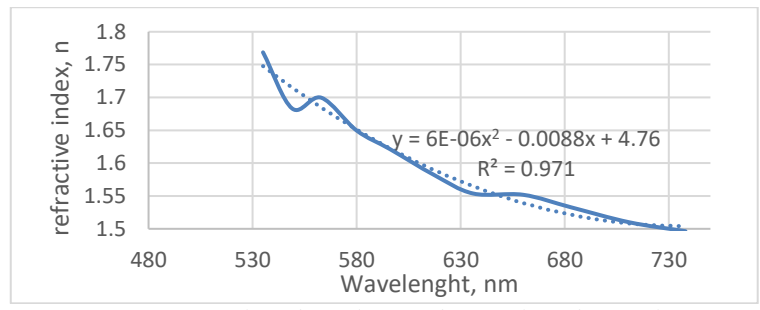


Figure 11. Plotted n values of diffuser liquid crystal.

Refractive index measurement curve below 530 nm starts to have more interference, so 535 nm limit was used for curve estimation. The parabolic curve shape is in agreement with measurements for other LC mixtures in literature [10].

The determined LC layer thickness, 3.0 μ m is larger than spacers 2.7 μ m, used for LC layer thickness control, so we conclude that cells have little excess of LC volume and glass is not completely resting on spacers. Spectrometric results correlate with model calculations, so model can be used for other form factor diffuser LC layer thickness control.

3.2. Diffuser solid state material interaction with electromagnetic waves

3.2.1. Optimization of antireflective film stack on outer surface of diffuser

The primarily aim of the work is to increase transmittance of the diffuser stack. To achieve this, we need to take care of air-glass reflections for outer diffusers. From the experience with larger size diffusers, commercial broad band antireflective (BBAR) coating can decrease ~7% of reflections from the air-glass boundaries for single diffuser, so we can expect similar gain. In addition, we can optimize BBAR coating even further by using own PVD coater.

Commercially available BBAR is optimized for general use at broad wavelength range but in our system, reflection at projector RGB wavelengths is important. COMSOL Multiphysics software was used to model reflection from glass surface by using *Thin dielectric layer* feature and then auxiliary parametric sweep for optimization mode. This yielded one stack for experimental trials – CS_2 with less reflection in lower wavelength region and, alternatively by using Optilayer program, CS_3 with flatter curve and lower normalized reflection (0.7% vs 1.2%), see Table 3 and Figure 12. Commercial

stack was also modelled under name CS_1. For the model, glass n-k data dispersion was used and for coatings - n values at 550 nm wavelength.

Table 3 Antireflection stack models and experimental results

		Model	Experime	ntal results	
Stack	Commer- cial	CS_2	CS_3	BBAR_2	BBAR_3
Nb ₂ O ₅ , nm	10	10	12	11	12
SiO _x , nm	40	40	32	39	32
Nb ₂ O ₅ , nm	110	120	115	119	115
SiO _x , nm	80	90	88	85	88
Average reflection, visible range	1.3%	0.6%	0.6%	4.8%	4.8%
Reflection at 450 nm	0.9%	0.3%	0.5%	5.0%	6.9%
Reflection at 532 nm	0.4%	0.6%	0.4%	4.9%	4.6%
Reflection at 635 nm	0.2%	0.3%	0.3%	4.2%	4.5%
Reflection sum at RGB	1.57%	1.18%	1.19%	14.1%	16.0%

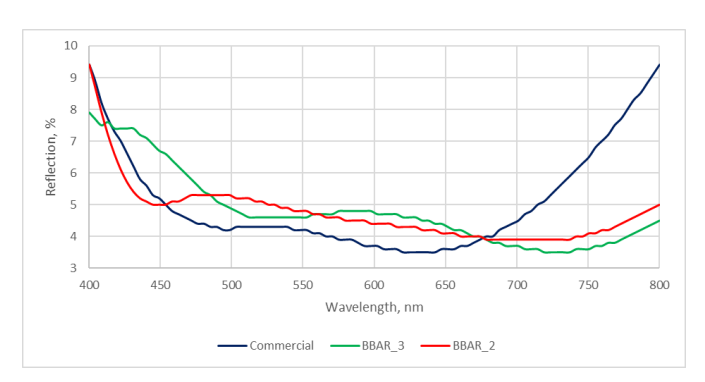


Figure 12 BBAR_2 and BBAR_3 coating reflectance spectra, taken with Ocean Optics Flame T spectrometer compared to commercial AR.

Model in Optilayer software with n-k dispersion data was used for comparison purposes. When comparing the results, we find that even Optilayer software

cannot predict precise curve but improved COMSOL model provide more closer results, see Figure 13.

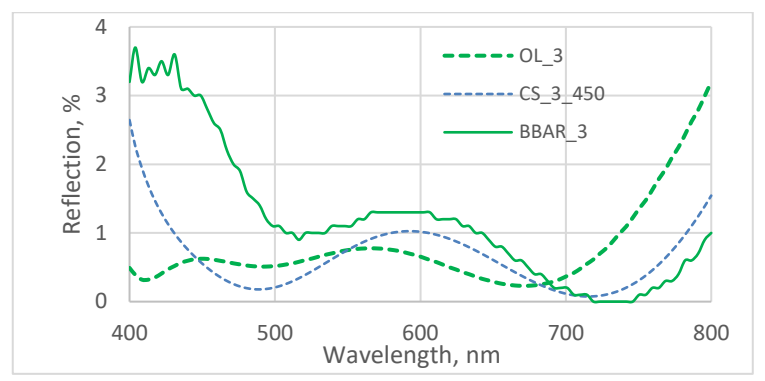


Figure 13 BBAR_3 coating comparison with various models. Blue- COMSOL with n values at 450nm, green- Optilayer with n,k dispersion values.

For wavelength specific applications, like optic chip in the RGB laser projection system, COMSOL model can provide effective input for AR layer coating optimization experiments. As the result, thickness of individual layers was adjusted, resulting in improved AR properties.

3.2.2. Optimization of transparent conductive layer

The aim of the experiments was to increase transmittance by using thinner ITO layers with improved conductivity as well as use low temperature process for deposition. Number of experiments to improve ITO layer conductivity was carried out. ITO layer is sputtered on soda lime glass using FHR Line 2500H PVD machine by low temperature process, so post process temperature treatment is used. It was found that 30 min at 300°C are sufficient for 1.6% transmittance improvement and nearly doubling the conductivity of 107 nm thick layer.

It would be more effective if high temperature treatment was done during process thus saving time and energy. In the next step, sputtering process temperature was increased and process conditions optimized further. ITO sample, was prepared by increasing sputter chamber heater temperature to 150°C. No improvement was obtained over postprocess temperature treatment method. ITO deposition parameters for 107 nm thick layer were varied with different partial oxygen content in reactive atmosphere. It was found, that the optimum oxygen content is achieved at oxygen flow of 18 sccm (standard cubic centimeters per minute), as it offers best transmittance and conductivity.

Increasing oxygen flow rate (hence more oxygen content in reactive atmosphere) improves transmittance but significantly lowers conductivity.

We can see that for low temperature deposition process, 120nm ITO coating is needed to reach 80 ohm/sq conductivity compared to high temperature deposition process, (30nm, 80 ohm/sq, n=1.82, supplier Token) and its refractive index is also higher, see *Figure 14*. Observed improvement of conductivity and transmittance after temperature treatment can be used to improve layer properties, by its effect on n and k values, reducing layer absorbance. This must be taken into account when designing all layer stack.

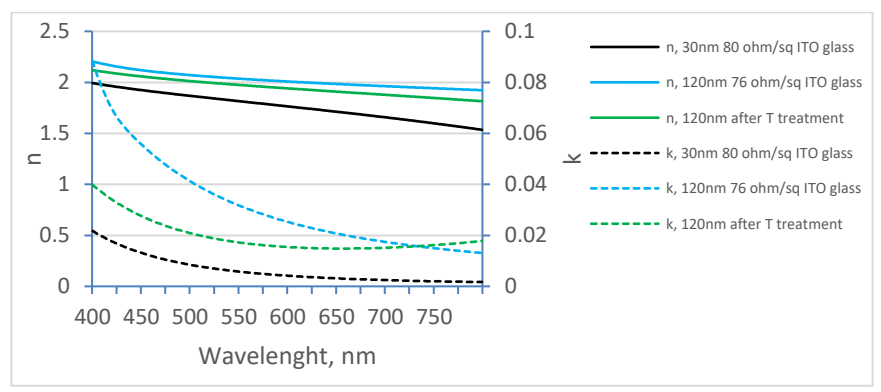


Figure 14 Refractive indexes n, k of ITO glass samples

3.2.3. Dielectric coating

Next, we will need to increase transmittance of each individual diffuser. As a rule of thumb, each 0.1% improvement for single diffuser transmittance will lead to 0.3% transmittance gain for the laminated stack, so to get 1% improvement we need to increase transmittance of single diffuser by 0.4%.

This can be done by matching refractive index of internal layers (stack). Reduction of layer number is secondary aim, as fewer number will lead to more efficient production if single layer could be used index matching and LC alignment. We have possibility to use sputtered SiO_x coating with refractive index of 1.51. In order to improve diffuser transmittance, refractive index should be matched to adjacent layers: ITO (1.82) and LC (1.71). The standard thickness for SiO_x coatings is 260nm, the value experimentally found for larger size diffusers that has optimum compromise between transmittance and dielectric breakdown for 300x400mm displays. For micro-diffusers, dielectric breakdown is less common due to smaller active area so thickness can be adjusted.

The next experiment was to find out how much dielectric coating on top of ITO, SiO_x , refractive index can be changed to improve transmittance even further by closer index matching between stack layers. Industrial coater FHR Line2500.H has limited options for changing sputter process conditions. Among them, most likely oxygen flow and surface temperature could provide larger impact on coating properties. No significant change to refractive index was detected. Pilot scale SiO_xN_y coatings were prepared on soda-lime glass lime using pulsed DC magnetron sputtering system in $Ar/O_2/N_2$ atmosphere that consists of vacuum coater SAF 25/50, TruPlasma DC Series 4000, TRUMPF Hüttinger. Transmittance spectra of $SiO_xN_y/glass$ samples measured by Agilent Cary 7000 spectrophotometer are given in Figure 15. Transmittance decreases with refractive index increasing. Lowest total transmittance is observed in sample with highest refractive index (S280), but at 550 nm transmittance for this sample is similar to other $SiO_xN_y/glass$ samples.

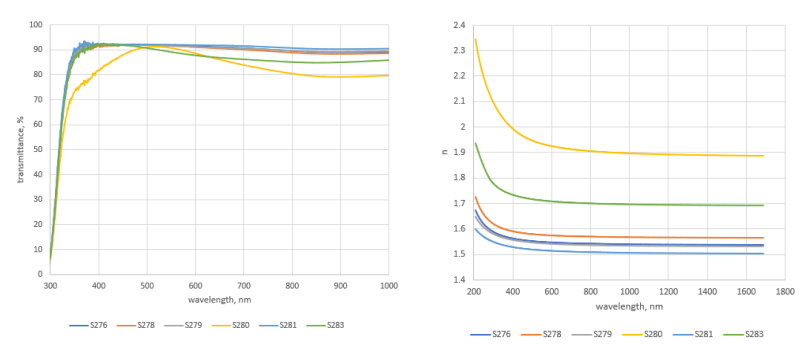
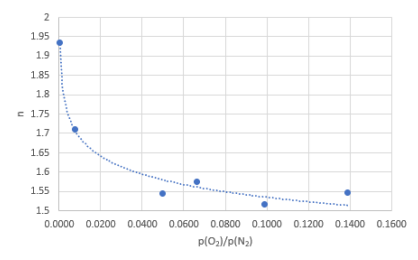


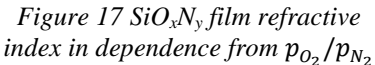
Figure 15 SiO_xN_y/glass samples transmittance spectra

Figure 16 SiO_xN_y/glass ellipsometry measurements

Ellipsometry measurements were taken with spectral ellipsometer Woollam RC2 – XI at incident light angles of 45, 50, 55, 60, 65 and 70 degrees. Spectral ellipsometer measurements for all samples are given in Figure 16. It is clearly seen that using this technology it is possible to adjust $\mathrm{SiO_xN_y}$ coating refractive index. The refractive index curve (at 550 nm) as a function of the ratio of the partial pressures of oxygen and nitrogen is shown in Figure 17.

XPS measurements were carried out and dependence of the refractive index on the nitrogen content in the SiO_xN_y film is given in Figure 18. Absolutely linear dependence of the refractive index on the nitrogen content in SiO_xN_y film is achieved.





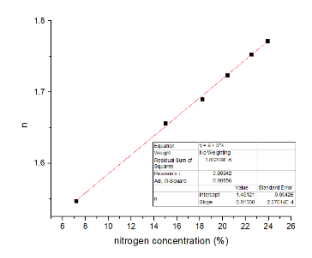


Figure 18. Refractive index of the SiO_xN_y film depending on the nitrogen content.

To evaluate dielectric coating optical thickness impact on diffuser transmission, full display stack was modelled with Optilayer and CODE V software, using layer materials n-k data. Thick layers (glass, LC) were defined as non-coherent to avoid interference. Modelling using Optilayer software predict that n=1.75 would give lowest reflectance, see Figure 19.

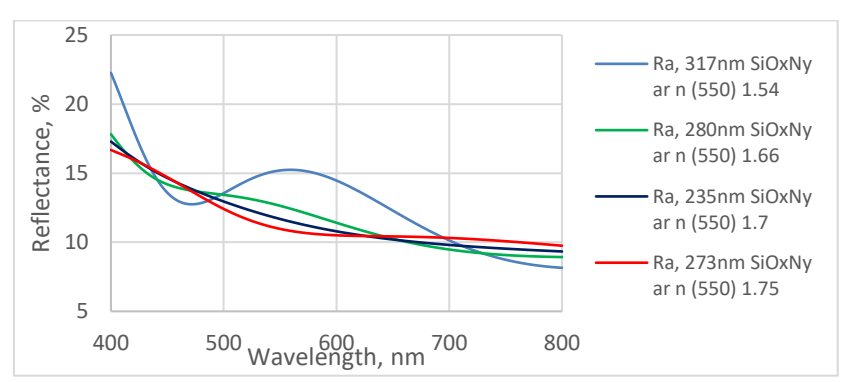
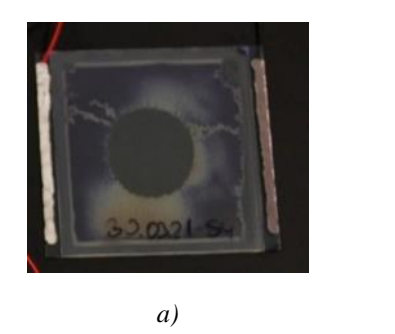


Figure 19 Optilayer simulation of diffuser reflectance dependence from various SiO_xN_y layers

Experimental diffusers using modelled input were prepared. For SiO_xN_y reference $196nm\ SiO_x$ coated samples were used. Note that because SiO_x coated samples were not deactivated by high temperature treatment, so after assembly of samples into cells, they have developed active unfilled area defect, see *Figure 20*.





b)

Figure 20 Empty void defects for a) SiO_x coated samples and absence of them b) for SiO_xN_y

This defect is identical to large size diffusers where temperature untreated SiO_x coatings are used. There to avoid this defect, most likely due to very active SiO_x surface, coating should be treated 2h at $300^{\circ}C$. On the contrary, SiO_xN_y samples did not had this defect, so temperature treatment step is not necessary. Some spots with different LC alignment can be observed but none of the void defects. The overview is given in Table 4. From the electro - optical test results, one can see that best open state transmittance is obtained for n=1.66. Note that the raise time is faster due to changed dielectric properties and thinner coating.

Table 4 E-O results for diffusers with SiO_xN_y coatings

Coating	n	Thick-	Max	E-O tes	st, %	E-O	test
	(550	ness,	trans-			(speed	d), μs
	nm)	nm	mission, %	Open	Close	Fall	Rise
SiO _{1.84}	1.51	196	87.8	88.8	12.3	695	1030
SiO _{1.14} N _{0.62}	1.75	276	88.9	88.8	8.3	735	463
SiO _{1.40} N _{0.42}	1.66	287	89.4	90.8	8.6	735	463

Optilayer software predicted n=1.75 to give higher transmittance in open state but in practice we see than n=1.66 is better, see Figure 21.

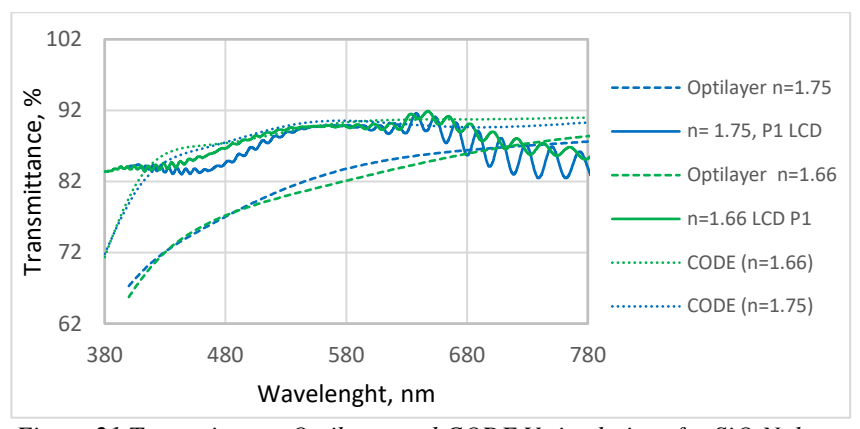


Figure 21 Transmittance Optilayer and CODE V simulations for SiO_xN_y layer combinations vs real results (LCD)

Alternative modelling using CODE V software was also done and its result suggests that n= 1.66 is better that agrees with practical results, so most likely its model is more appropriate as it takes into account k values, that are nonzero for coatings with n above 1.7 at 550nm, see Figure 22.

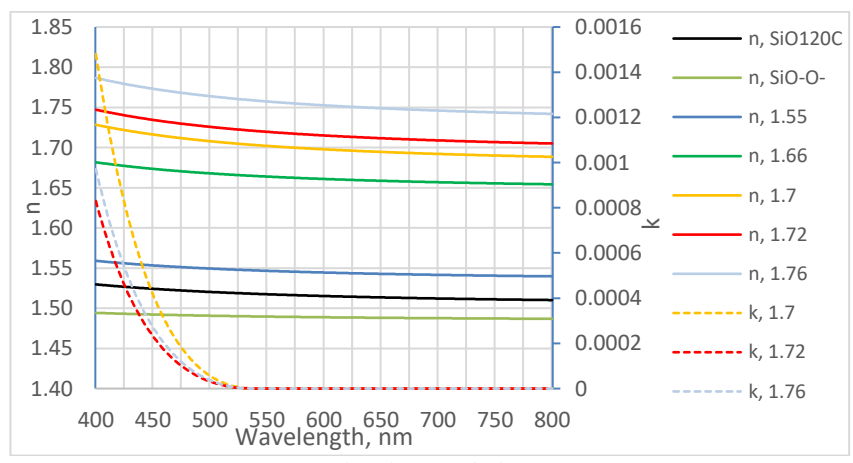


Figure 22 n, k values of dielectric coatings

Finding optimum mode by CODE V software predicts n=1.55 and 200nm thickness. Samples were made and while results are better than reference but do not improve previously reached results, see *Table 5*.

Table 5 E-O results for diffusers with predicted optimum SiO_xN_y coatings

Coating	Approximate thickness, nm	E-O test Open-close	E-O test, speed Fall-raise	n at 550 nm
SiO _{1.77} N _{0.21}	187+195	89.1-9.1%	671-735	1.54
SiO _{1.77} N _{0.21}	193+197	89.4-9.2%	663-862	1.54

Obviously, for stack transmission optimization, coatings up to n=1.7 at $550\,$ nm should be used as they have k value of zero. 280-290nm thick SiO_xN_y coating with n=1.66 will give best results for diffuser transmission. Thinner coating will increase risk of dielectric breakdown but in principle, when coating quality is improved, may be used for diffusers.

Coating process was set on larger scale FHR Line2500.H sputtering machine based on SiOx process settings but adding O_2 to N_2 process gas. By varying process gas ratio, coatings with different refractive index were achieved with almost liner dependence, see *Figure 23*.

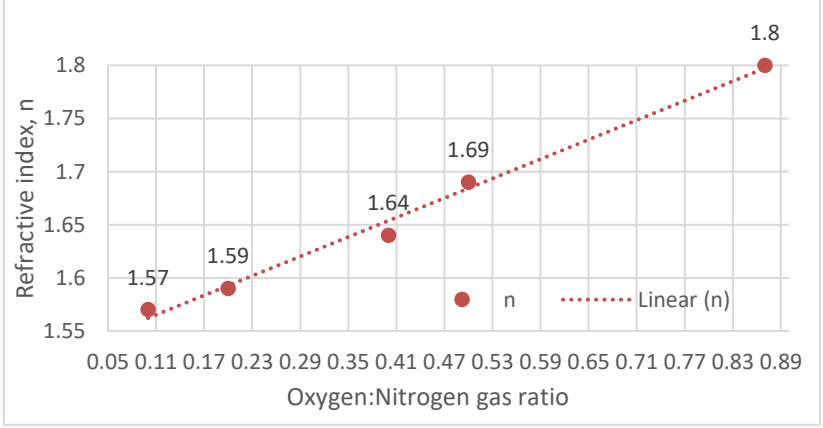


Figure 23 Refractive index (at 550nm) dependence on process gas oxygen: nitrogen ratio in FHR machine. Higher ratio corresponds to more nitrogen.

For diffusers, coating properties can be tuned with oxygen: nitrogen ratio in reactive sputtering, the preference given for 0.5 oxygen: nitrogen ratio (if ITO layer have refractive index closer to 2) or 0.2 (if high temperature deposited ITO with refractive index 1.8 is used).

3.3. Single diffuser and multifocal diffuser build up

The next aim is to make micro-diffuser with minimum spacer density or, preferably, without spacers at all. From substrate deflection formula, one can calculate that 0.11 spacers/mm² are needed to avoid potential substrate bow more by 10% between 8µm spacers. This is very low number. For vacuum capillary fill (VCF) process, after the LC is filled, the excess of LC is squeezed out to get 10% compression, typical pressure is 0.04 N/mm². Yet, during LC capillary filling process itself, 0.01 N/mm² transient pressure is applied, so calculation by using formulas in literature, suggests that there should be at least two spacers for square mm to prevent cell total collapse and spacer will be temporally compressed by 46%. However, we do not know the value at which elastic deformation ends, so it is not clear what the final spacer shape will be. Also, influence of gasket as relatively incompressible support not far away, is not taken into account.

For one drop fill (ODF) process, the pressure during assembly is lower – only 0.0005 N/mm² and when atmospheric pressure is renewed, the pressure is taken up by LC, so the bow is actually limited by LC volume in diffuser cell. 0.5 spacers/mm² could be realistic goal based on static modelling.

Dynamic calculations would be more precise taking into account gasket region with spacers mixed in and area outside the cells without LC and spacers. Full 3D model of 33x22mm cell was too complicated to build in COMSOL as computation requirements are very high due to multiple micron sized object meshing. However, it is possible to simplify model by calculation of glass displacement in 2D model, taking into account glass and spacer properties.

From the modelling results we can see that spacers are necessary and the cell will collapse under applied pressure without them. To avoid gap deviation more than our specified limit ($\pm 10\%$) we need at least 1 spacers per mm². In the same time, we must acknowledge that spacer spray is random process and areas of lower density will occur, so cell even with 4 spacers per mm² may not be achievable. During production, cell must undergo several steps with different applied pressure. For 33x22 mm cell with 8 μ m spacer density of 1 spacer/mm², cell gap change can be calculated for each step, see Table 6.

Table 6 Cell gap change during process steps for 8um spacers

Process step	Pressure N/mm ²	Gap change, µm
Without load	Glass own weight	0.001
Assembly in air	0.0004	0.06
Curing in multipress	0.005	0.35
Capillary vacuum fill	0.010	0.06
End seal press	0.014	0.08

Low spacer density, like 1 spacer/mm², could be achievable with photo spacer process, when each spacer is formed in prescribed place. If we use random spacer spray, we must take into account that some spacers might be missing due to clustering effect, see Figure 24.



Figure 24 Spacer distribution pattern showing cluster of five spacers and unpopulated areas nearby

The influence of some missing spacer in the middle of the cell is larger than nearer to cell side, where it is stabilized by gasket. We find that absence of 6 spacers will result in cell gap collapse, see Figure 25.

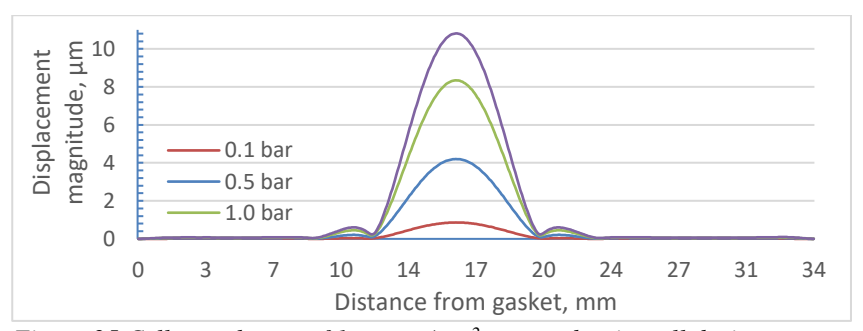


Figure 25 Cell gap change of 1 spacer/mm² spacer density cell during process steps with 6 spacers missing in the center.

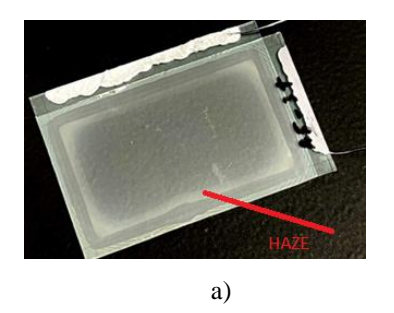
We can conclude that theoretically, spacer density below 1 spacer/mm² can be achievable for photo spacers but for conventional sprayed spacers, spacer densities must be higher to ensure that there are no unsupported areas. It is more a safety factor, and how close we can get to theoretical modelled density, must be determined experimentally. We can assume that at least safety factor of 5-10 is needed. In order to find optimum spacer density and test modeling validity, several 22x15mm series with different 8um spacer density were manufactured. The results show close state transmittance decrease for lower spacer density due to thinner cell gap that leads to undesired loss of contrast,

see *Table 7*. So, for vacuum capillary method (VCF) method, minimum spacer density is above 100 pcs/mm².

Table 7 Spacer density impact on VCF diffuser E-O properties

Panel	Spacer density, pcs/mm ²	Open, %	Close, %	Fall time, µs	Rise time, µs
P3-2	130 ±20	89.1	18.8	658	1216
P3-4-1	37 ±10	89.6	22.4	674	874
P2-2-1	24 ±5	89.5	25.1	678	759
P2-4-1	8 ±2	88.7	38.4	710	335
	0.5 ±1	Half of area is not filled with LC			
	Spacerless, 0	Half of are	a is not f	illed with Lo	C

During E-O tests, 10 V above switching threshold in open state, haze zone was observed near gasket, see Figure 26. At first, it was attributed to thicker cell gap as predicted by COMSOL model, as gap is thicker near the gasket. However, under microscope, it can be observed that in this region, LC have different orientation than in middle of the cell, that led to hypothesis that SiO_x surface near gasket are somehow influenced by gasket. Similar observation was reported in literature[27], only for inorganic alignment coatings. It is supposed that active SiO_x surface absorbs hydrocarbons from gasket material during manufacture that leads to change of surface alignment for LC. In our case, this haze zone can be countered by higher driving voltage, i.e. raising electric field intensity by 20-30V, necessary to overcome additional alignment force.



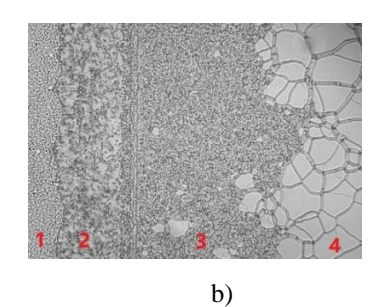


Figure 26 ODF cell (33x22mm) in diffuse state during E-O test. a) "frame" like haze zone near gasket b) magnified haze zone, 1 – gasket, 2 – undriven area outside LC, 3- scattering FC zone, 4- transparent ULH zone

Further reduction of spacer density was done for cells made by ODF method with selected underfill ratio. This time, SiO_x coating was substituted by index matched SiO_xN_y coating. The cells were examined under polarizer to observe gap homogeneity, see *Figure 27*. Densities above 5 spacer per mm² have good uniformity.

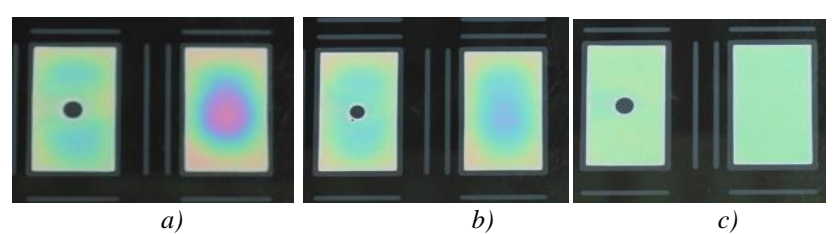


Figure 27 Cell gap homogeneity of ODF cells with spacer density: a) spacerless, b) 2 spacer/mm², c) 5 spacer/mm². Cells on the left have support dot from the gasket material in the middle.

From the electro-optical test results, see

Table 8, we can see that most stable results are obtained for 28 spacer/mm² density and while 5 spacer/mm² had good uniformity of cell gap, it is thinner.

Table 8 E-O test results for ODF cells with various spacer density

Spacer density,	Open,	Close,	Close,	Fall	Rise time,
pcs/mm ²	%	%	STDEV%	time,	μs
				μs	
99 ±16	91.0	21.5	0.6	720	1076
50 ±4	91.2	20.4	0.5	737	998
28 ±1	91.4	19.7	0.4	727	1059
5 ±1	91.5	23.5	0.5	741	797
2 ±1	91.3	26.0	1.1	750	647
none	91.5	35.0	5.1	785	385

Haze zone near gasket was minimal, confirming that less active SiO_xN_y is better, see *Figure 28*.

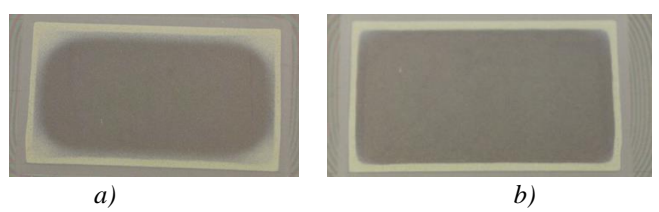


Figure 28 Haze zone intensity near gasket is higher for cells with a) SiO_x than b) SiO_xN_y , coating

Multifocal liquid crystal diffusers from 4 laminated units using WR5500 glue was made, see *Figure 29*, are successfully manufactured and used in Lightspace Technologies AR-HMDs models.

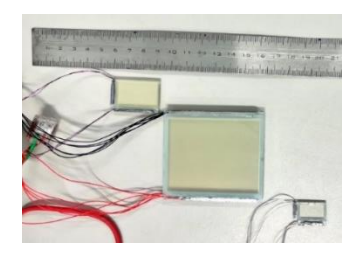


Figure 29 Different form factor multifocal diffusers. Larger prototype from beginning of this work, shown in the middle.

4. Conclusions

Optimum material combination and structural design for diffusers have been found by using numerical modelling methods that decreased amount of experimental work and saving resources. COMSOL Multiphysics were used to build appropriate models that were validated by experimental results and, where applicable, by optical design software.

Key characteristics of a cholesteric liquid crystal diffuser, which is a part of multifocal liquid crystal diffuser, were evaluated:

- The dynamics of the relaxation process from homeotropic to focal conic transition was addressed, stressing on the influence of the different factors such as dopant concentration, electronic driving, and surface anchoring conditions;
- The dependence of the scattered light effectiveness of the diffuser on factors such as pointed above was also analysed;
- The appearance of a transient state during the relaxation process from homeotropic to focal conic state, revealing its possible origin.

For instance, increasing the concentration of a chiral dopant used in the PFLC diffuser shortens cholesteric pitch and decrease switching time from homeotropic to focal conic state at the expense of increased driving voltage. However, the dependency of fall time *vs* concentration has a pronounced minimum after which increasing concentration of chiral additive increases the switching time, while decreasing the effectiveness of the diffuser element's light scattering power. For one of the highest HTP dopants, the optimum concentration is found to be about 2.5%.

The surface anchoring condition also has an effect on characteristics of diffusers. The light-scattering characteristics can be facilitated by antiparallel surface alignment, which was shown to improve close state transmission nearly twice in comparison to homeotropic alignment while increasing switching time from homeotropic to focal conic by 30%. The influence of the anchoring conditions is most prominent in the cells with thinner cell gap. Also, the close state transmittance value can be improved by yellow dye addition.

Transient increase of transmittance during change from transparent (homeotropic) state to diffuse (focal conic), cannot be explained by transient planar state, characteristic to PDLC, as there are no evidences in reflective and capacitive properties. Instead, uniform lying helix state formation is proposed. One possible way to remove it is to apply electric field with form of continuous decrease of the applied voltage (ramp) to the diffuser rather than a sudden switch-off the voltage.

Diffuser type liquid crystal layer thickness measurement method based on capacitance measurements was developed and validated. COMSOL Multiphysics model have been used to compute capacitance values. Capacitance method has been validated by spectroscopic thickness measurement method for LC with known refractive index. Proposed LC layer thickness control method has been approbed for use in inline LCD production. Moreover, obtained value of layer thickness by this method was used to determine refractive index of novel liquid crystal mixture for diffuser (light scattering) LC. Knowledge of refractive index allows further optimization of LCD cells in future by index matching.

Transmittance values for multifocal diffuser have been improved by optical stack optimization. Thickness and properties of internal coating facing active LC were optimized for better optical performance. SiO_xN_y coating was developed for index matching dielectric layers as its refractive index can be easily adjusted by varying oxygen: nitrogen ratio during sputter process. In the same time it serves the purpose of LC alignment layer and prevent dielectric breakdowns. Most notably less diffuser cell defects are observed as SiO_xN_y surface is less active in comparison to sputtered SiO_x .

Designated goal for spacerless diffuser design cannot be implemented and there is minimum necessary spacer density. With less spacer density the distances between spacers are becoming too large and substrate deflection start to play more significant role. In models based on theoretical assumptions and formulas we suppose that surfaces are perfectly flat and spacer distribution is ideal. In reality, assembly machine surfaces have 50µm flatness and for spacer wet spray method precise location of spacers cannot be controlled, especially when lower densities are used. It is not possible to decrease spacer density for capillary fill method. To achieve stable results, at least 25 pcs/mm² are required for ODF method. If lower density is required, it can be done by selecting larger diameter spacers thus compensating their ~20% compression or other method (photo spacers) should be chosen.

Within in this thesis presented investigation, substantial improvement of multifocal liquid crystal diffusers properties (see *Table 9*) have been reached and developed diffuser used in AR-HMDs.

Table 9 Achieved specification results of the work

Specification	At the start	Goal	Achieved
	of work		results
Size, active area	62x49 mm	26x15	26x15
		mm	mm
		16x9 mm	16x9 mm
Distance between active LC	1.1mm	0.66 mm	0.66mm
layers			
Number of layers	47	39	39
Inactive elements in size of	136 pcs/mm ²	0-100	25
8µm		pcs/mm ²	pcs/mm ²
Total set transmission in	78%	82%	85%
open state			
Individual unit transmission	20.4%	19%	18.3%
in diffuse state*			
Individual unit transmission	89.3%	90.5%	92.3%
in open state*			

^{*-} without BBAR coatings on air/glass boundary.

Main thesis

- After fast removal of electric field in short pitch polymer free cholesteric liquid crystal systems transition from homeotropic to focal conic state occurs via transient uniform lying helix formation.
- Sputter coated SiO_xN_y film could be used to simultaneously fulfill four functions —passivation of conductive layer, refractive index matching, dielectric insulation and serve as alignment layer, besides, it effectively replaces two layers typically used in LC technology a silica based inorganic protective (hardcoat) layer and organic dielectric/alignment layer.
- Developed technology is used to produce miniature multi-layer liquid crystal diffuser with advanced electro-optical properties that meet the requirements of augmented reality displays.

Authors list of publications

Granted and *submitted* patents:

- 1. Osmanis, I. Ozols, A., Osmanis, K., Zabels R., Optical display arrangement and method of operation, US 2019 / 0146232 A1, May 16, 2019
- 2. Osmanis, I., Osmanis, K., Narels, M., Gertners, U., Zabels, R., Smaukstelis, A., Ozols, A., Table top volumetric display apparatus and method of displaying three dimensional image, US 10,726,751 B2, Jul 28, 2020
- 3. Osmanis, I., Narels, M., Osmanis, K., Ozols, A., Gertners, U., Zabels. R., Display system for generating three-dimensional image and method therefor, US 17081183 (Application Number), Published: 28.04.2022.
- 4. Osmanis, I., Osmanis, K., Zabels, R., Narels, M., Gertners, U., Valters, G., Ozols, A., Near-eye display apparatus and method of displaying three-dimensional images, US 17109441 (Application Number), Published: 01.04.2021.
- 5. Ozols, A., Osmanis, I., Osmanis, K., Narels, M., Mozolevskis, G., Zabels, R., Improved liquid crystal cell, US17/404,392 (submitted August 17, 2021)
- 6. Gertners, U., Osmanis, I. Narels, M., Ozols. A., Balode, S., Zabels R., Optical element for expanding and uniforming beam of light, US17/514,679 (submitted October 29, 2021)
- 7. Osmanis, I., Gertners, U., Osmanis, K., Narels, M., Greitans, M., Ozols, A., Balode, S., Zabels, R., Optical arrangement for expanding and uniformizing light beams, US17/581,169 (submitted January 21, 2022)

Publications:

- 1. Zabels, R., Osmanis, K., Narels, Ozols, A., Osmanis, I., AR displays: Next-generation technologies to solve the vergence-accommodation conflict, Applied Sciences (Switzerland), 2019, 9(15), 3147, DOI:10.3390/app9153147.
- 2. Osmanis, K., Zabels, R., Ozols, A., Narels, M., Osmanis, I., Stereoscopic ar displays towards solid-state multi-focal architecture, Digest of Technical Papers SID International Symposium, 2020, 51(1), pp. 1638–1641, DOI:10.1002/sdtp.14208
- 3. Zabels, R.; Osmanis, K., Ozols, A.; Narels, M.; Gertners, U.; Smukulis, R.; Osmanis, I.; "Volumetric technology: enabling near-work compatible AR displays," Proc. SPIE 11304, Advances in Display Technologies X, 113040E (26 February 2020), DOI: 10.1117/12.2544891.
- 4. Ozols A.; Zutis E.; Zabels R.; Linina E.; Osmanis K.; Osmanis I.; "Fast-switching liquid crystal diffusers: outlook on optical properties and applicability in volumetric display architecture," Proc. SPIE 11788, Digital

- Optical Technologies 2021, 117880U (20 June 2021), DOI: 10.1117/12.2594147.
- 5. Ozols, A.; Mozolevskis, G.; Letko, E., Rutkis, M.; Zabels, R.; Linina, E.; Osmanis, I.; "Sputtered SiOxNy thin films: improving optical efficiency of liquid crystal diffuser elements in multi-focal near-to-eye display architecture," Proc. SPIE 11872, Advances in Optical Thin Films VII, 118720I (12 September 2021), DOI: 10.1117/12.2596885.
- 6. Ozols, A.; Mozolevskis, G.; Zalubovskis, R.; Rutkis, M.; "Development of liquid crystal layer thickness and refractive index measurement methods for scattering type liquid crystal displays", Latvian Journal of Physics and Technical Sciences, vol.59, no.4, 2022, pp.25-35. https://doi.org/10.2478/lpts-2022-0031.
- 7. Ozols, A.; Linina, E.; Zabels, R.; Komitov, L. Evaluation of the Characteristics of Cholesteric Liquid Crystal Diffuser Element Applied in Multi-Focal Display Architectures. Crystals 2022, 12, 733. DOI: 10.3390/cryst12050733.

Conferences:

- A. Ozols, G. Mozolevskis, E. Letko, M. Rutkis, R. Zabels, E. Linina, I. Osmanis, "Sputtered SiOxNy thin films: improving optical efficiency of liquid crystal diffuser elements in multi-focal near-to-eye display architecture," SPIE Optical Systems Design, 2021, Online Only.
- A. Ozols, E. Zutis, R. Zabels, E. Linina, K.Osmanis, I. Osmanis, "Fast-switching liquid crystal diffusers: outlook on optical properties and applicability in volumetric display architecture," SPIE Digital Optical Technologies, 2021, Online Only.
- A.Ozols, "What silica-based thin films could do for augmented reality displays?", FM&NT NIBS 2022.
- A.Ozols, E.Linina, R.Zabels, "Optimization of Total Light Transmittance for AR/VR Displays by Use of Silica Based Thin Films", Eurodisplay 2022.

References

- [1] R. H. Chen, *Liquid crystal displays: fundamental physics and technology*. Wiley, 2011.
- [2] A. K. Jain and R. R. Deshmukh, "An Overview of Polymer-Dispersed Liquid Crystals Composite Films and Their Applications,"

- Liquid Crystals and Display Technology, Oct. 2020, doi: 10.5772/INTECHOPEN.91889.
- [3] D. K. Yang and S. T. Wu, "Fundamentals of Liquid Crystal Devices," *Fundamentals of Liquid Crystal Devices*, vol. 9781118752005, pp. 1–570, Dec. 2014, doi: 10.1002/9781118751992.
- [4] J. Chen, W. Cranton, and M. Fihn, "Handbook of visual display technology," *Handbook of Visual Display Technology*, pp. 1–3564, Jan. 2016, doi: 10.1007/978-3-319-14346-0.
- [5] P. E. Watson, "The homeotropic to planar transition in cholesteric liquid crystals /," Kent State University, 2000. Accessed: May 08, 2022. [Online]. Available: https://www.researchgate.net/publication/35743508_The_homeotropic_to_planar_transition_in_cholesteric_liquid_crystals?msclkid=e4c4c694cecd11ecb20532f0dec3ecf1
- [6] A. Sullivan and JOHNSON SARA L, "3D display devices with transient light scattering shutters," 20020113753, 2002
- [7] A. Ozols, E. Zutis, R. Zabels, E. Linina, K. Osmanis, and I. Osmanis, "Fast-switching liquid crystal diffusers: outlook on optical properties and applicability in volumetric display architecture," in *Digital Optical Technologies* 2021, Jun. 2021, p. 26. doi: 10.1117/12.2594147.
- [8] S. Palmer and B. Backlund, "Polymer-free Cholesteric Textured (PFCT) Liquid Crystal Optical-shutters," Borlange, 2005.
- [9] F. Bruyneel, "Method for measuring the cell gap in liquid-crystal displays," *Optical Engineering*, vol. 40, no. 2, p. 259, Feb. 2001, doi: 10.1117/1.1337036.
- [10] J. Li, C. H. Wen, S. Gauza, R. Lu, and S. T. Wu, "Refractive indices of liquid crystals for display applications," *IEEE/OSA Journal of Display Technology*, vol. 1, no. 1, pp. 51–61, Sep. 2005, doi: 10.1109/JDT.2005.853357.
- [11] E. Nitiss, R. Usans, and M. Rutkis, "Simple method for measuring bilayer system optical parameters," https://doi.org/10.1117/12.922317, vol. 8430, pp. 380–390, May 2012, doi: 10.1117/12.922317.
- [12] S. Valyukh, S. Sorokin, and V. G. Chigrinov, "Inline Quality Control of Liquid Crystal Cells," *Journal of Display Technology*, vol. 11, no. 12, pp. 1042–1047, Dec. 2015, doi: 10.1109/JDT.2015.2434939.
- [13] A. M. Mandong and A. Uzum, "Fresnel calculations of double/multi-layer antireflection coatings on silicon substrates," *Research on Engineering Structures and Materials*, vol. 7, no. 4, pp. 539–550, 2021, doi: 10.17515/RESM2020.241EN1217.

- [14] B. S. Chiou and J. H. Tsai, "Antireflective coating for ITO films deposited on glass substrate," *Journal of Materials Science: Materials in Electronics 1999 10:7*, vol. 10, no. 7, pp. 491–495, 1999, doi: 10.1023/A:1008924018328.
- [15] G. H. Guai, Q. L. Song, Z. S. Lu, and C. M. Li, "Effects of multiple heat treatment cycles on structure, optical and electrical properties of indium-tin-oxide thin films," *Surface and Coatings Technology*, vol. 205, no. 8–9, pp. 2852–2856, Jan. 2011, doi: 10.1016/J.SURFCOAT.2010.10.062.
- [16] Nissan Chemical, "LCD coating material data sheet." 2012.
- [17] S. v. Pasechnik, V. G. (Vladimir G.) Chigrinov, and D. v. Shmeliova, *Liquid crystals: viscous and elastic properties*. Wiley-VCH, 2009.
- [18] G. Mozolevskis, I. Sekacis, E. Nitiss, A. Medvids, and M. Rutkis, "Dielectric breakdown of fast switching LCD shutters," *Advances in Display Technologies VII*, vol. 10126, p. 1012607, Feb. 2017, doi: 10.1117/12.2252492.
- [19] H. S. Vanegas, M. Pinzón, J. E. Alfonso, J. J. Olaya, and C. Pineda-Vargas, "Chemical characterization and optical properties of SiOxNy films deposited on common glass substrate," *Materials Express*, vol. 6, no. 3, pp. 295–299, Jun. 2016, doi: 10.1166/MEX.2016.1306.
- [20] H. Kamiya *et al.*, "56.3: Development of One Drop Fill Technology for AM-LCDs," *SID Symposium Digest of Technical Papers*, vol. 32, no. 1, pp. 1354–1357, Jun. 2001, doi: 10.1889/1.1831814.
- [21] J. Souk, S. Morozumi, F.-C. Luo, and I. Bita, "Flat panel display manufacturing".
- [22] K. Hemanth Vepakomma, M. Pandey, T. Ishikawa, and R. Koona, "Paper No P41: Predicting Change in Cell Gap in LCD Panels Subjected to Touch Force," *SID Symposium Digest of Technical Papers*, vol. 44, pp. 144–147, 2013, doi: 10.1002/SDTP.23.
- [23] Cuypers Dieter, "Vertically aligned nematic liquid crystal microdisplays for projection applications," Gent University, 2005. Accessed: May 08, 2022. [Online]. Available: https://biblio.ugent.be/publication/470265?msclkid=261ab0f6cee111e cb7a1f51f2fb70ef2
- [24] van de J. Steen, "Design of LCOS microdisplay backplanes for projection applications," Gent University, 2006. Accessed: May 08, 2022. [Online]. Available: https://www.researchgate.net/publication/292348523_Design_of_LC

- OS_microdisplay_backplanes_for_projection_applications?msclkid=6 795e168cee111ecbeaaf5a7d943d1d3
- [25] G. Bodammer, D. W. Calton, and I. Underwood, "26.3: Investigation of the Bow of Silicon Backplanes for Microdisplay Applications," *SID Symposium Digest of Technical Papers*, vol. 32, no. 1, p. 439, 2001, doi: 10.1889/1.1831890.
- [26] C. Tani, "Phase Transition Temperature Dependence of Field-Induced Nematic-Cholesteric Relaxation Time," *Japanese Journal of Applied Physics*, vol. 18, no. 7, pp. 1387–1388, Jul. 1979, doi: 10.1143/JJAP.18.1387.
- [27] "[PDF] Assembly of an XGA 0.9" LCOS display using inorganic alignment layers for VAN LC | Semantic Scholar." https://www.semanticscholar.org/paper/Assembly-of-an-XGA-0.9%22-LCOS-display-using-layers-Cuypers-
- Doorselaer/d194c87a5b02c433d72314d6bd5108490355a5c7 (accessed May 09, 2022).